Broadband Strip-Transmission Line Y-Junction Circulators

J. W. SIMON, STUDENT MEMBER, IEEE

Abstract—Broadband circulators have been developed which operate below resonance and cover octave bandwidths in the frequency regions 0.6–8.0 Gc. The interrelationship of voltage standing-wave ratio (VSWR) and isolation between various ports is established without imposing symmetry. The fact that building a three-port circulator is essentially a matching process is used as a basis for a successful experimental development procedure. Empirically determined criteria for broadbanding are reported with particular emphasis placed on the discussion of optimizing saturation magnetization, linewidth, strip-transmission line parameters, and magnetic biasing field. The importance of having a ferrite with low dielectric loss tangent is also discussed. The empirical data are considered in light of theoretical work done in this laboratory and in light of the papers by Bosma.

Introduction

A NUMBER of papers [1], [2], [3] have been given which present in a general nature the methods utilized in making narrow-band circulators. Papers also have been presented which contributed to the fundamental understanding of junction circulators [4], [5], [6] but which do not deal specifically with the problem of broadbanding these devices. It is the aim of this paper to present useful information from these papers along with a large amount of empirical data which have been derived in the course of developing a number of broadband circulators.

These procedures have been applied successfully to the development of broadband strip-transmission-line Y-junction circulators for use over octave bandwidths in the frequency ranges of 0.6–1.2, 1.0–2.0, 1.5–3.0, 2.0–4.0, and 4.0–8.0 Gc.

The basis for this successful development procedure was suggested by the Humphrey and Davies paper [7], in which it was shown that the bandwidth could be extended by matching the ferrite element symmetrically using external reciprocal reactive networks. Using this approach, it was discovered that certain parameters (of the microwave structure and of the ferrite itself) could be varied to permit matching to be carried out with greater ease. Of greatest importance, an empirical evaluation of the impedance vs. frequency characteristics of the ferrite loaded junction revealed that adjustment of the saturation magnetization of the material could indeed be useful in creating the type of impedance response which realistically could be matched using microwave reactive structures. This evaluation was carried out in each band and resulted in the selection of a series of ferrite materials producing impedance characteristics suitable for broadband matching.

Thus, the operating bandwidth has been extended by utilizing external matching networks applied to ferrite loaded junctions that have been adjusted and optimized to reduce the difficulty of matching.

Empirical data are presented which indicate the relation between the saturation magnetization of the ferrite and the impedance vs. frequency characteristics in the bands previously mentioned. Also discussed in this regard are the effects of linewidth, width of the strip-transmission line, and the magnetic biasing field upon the impedance characteristics. Useful curves are presented which relate optimum ranges of $4\pi M_s$ and ferrite disk diameter to frequency. Methods of matching into the ferrite loaded junction are discussed, and the results are indicated for each band.

Technical Considerations

Broadband Approach

An important factor in the broadbanding effort was the recognition of the fact that the isolation of any port is dependent on the impedance match at the preceding port. It was verified experimentally, for a circulator operating in the low-loss mode port 1→port 2→port 3 →port 1 (1→2→3→1), that, when the power entered port 1, the isolation between port 1 and port 3 could be expressed by the following expression:

$$\text{Isolation } (1 \rightarrow 3) = 10 \log \frac{1}{\Gamma_2^2}$$

(provided that the normal situation exists in which power is not radiated), where Γ_2 = reflection coefficient of port 2.

This relation was found to hold accurately for VSWR values at least as high as 1.50 and does not require symmetrical matching.[1]

From this, it is clear that the basic problem of producing high isolation and low loss reduces to that of finding methods for matching into the ferrite loaded junction over a broad frequency spectrum.

Manuscript received June 5, 1964; revised January 26, 1965. This work was performed by Sperry Microwave Electronics Co. under Contract DA-36-039-SC-89214 sponsored by the U. S. Army Electronics Research and Development Lab., Fort Monmouth, N. J.

The author is with Scientific Atlanta, Inc., Atlanta, Ga. He was formerly with Sperry Microwave Electronics Co., Clearwater, Fla.

[1] A formal proof of this experimental result was derived using scattering matrix formulation and is provided in Appendix I.

This problem was approached in two ways: First, the impedance characteristics of the ferrite loaded junction were studied, while various parameters of the ferrite and microwave structure were varied. The result desired from this study was information leading to the development of techniques for simplifying the matching problem. Secondly, matching structures were developed to be used in conjunction with the forementioned characteristics.

Materials Selection

Since it was desired to discover what effect, if any, the saturation magnetization, $4\pi M_s$, of the ferrite material had upon the circulator impedance vs. frequency characteristics, it was necessary to choose a class of materials in which the dielectric constant, g factor, and linewidth ΔH could be held essentially constant while large changes in $4\pi M_s$ could be effected.

The basic material chosen for this evaluation was an aluminum substituted yttrium iron garnet. The properties of this garnet are well suited to this kind of test because of the following three factors:

1) The $4\pi M_s$ values can be varied from 1780 to 133 gauss for aluminum substitutions ranging from 0 to 27 per cent.
2) The material has a narrow linewidth that is approximately constant for aluminum substitutions from 0 to 27 per cent.
3) The value of the dielectric constant ϵ and the g factor change less than 10 per cent for aluminum substitutions from 0 to 25 per cent.

The particular $4\pi M_s$ values that were used for this test were 133, 200, 400, 500, 670, and 1005 gauss, respectively, which are listed in Table I along with properties and compositions.

TABLE I

ALUMINUM SUBSTITUTED YTTRIUM IRON GARNETS OF THE FORMULA $3Y_2O_3 \cdot 5[X\%Al_2O_3 \cdot (1-X)\%Fe_2O_3]$

Material No.	X	ΔH*	ϵ	$4\pi M_s$	°C Curie temp.	q factor	tan δ (less than)
1	27	40	14.25	133	136°	2.10	0.0002
2	25	40	14.38	200	140°	2.03	0.0002
3	20	40	16.0	500	150°	2.024	0.002
4	20	52	15.1	400	150°	2.03	0.0001
5	15	39	14.20	670	170°	2.02	0.0001
6	10	44	15.5	1005	200°	2.02	0.0001

* ΔH measured at 10 Gc.

PARAMETERS INVESTIGATION

Effects of $4\pi M_s$ in L and S Bands

Testing of ferrimagnetic materials with various values of $4\pi M_s$ was accomplished in the frequency bands 0.6–1.2, 1.0–2.0, 1.5–3.0, 2.0–4.0, and 4.0–8.0 Gc. For purposes of brevity, only the tests that were made in the 1.0–2.0 and 2.0–4.0 Gc bands will be described in detail here. Since the procedure is typical of all bands, only the final results will be presented in the 0.6–1.2, 1.5–3.0, and 4.0–8.0 Gc.

Material Evaluation, L-Band Region: The yttrium iron garnets listed in Table I as 1, 2, 4, and 5, respectively, were tested in this frequency band using a housing as shown in Fig. 1. These materials were tested at several magnetic fields, and the impedance characteristics were plotted on Smith charts.

The results of these tests are shown in Figs. 2 through 5. An interesting observation, which can be made from these Smith chart plots, is that, as the saturation magnetization of the garnet is increased, the impedance plot begins to coalesce. This suggests that the use of materials possessing high $4\pi M_s$ values would be advantageous. Because of low field loss considerations, however, only a limited increase in the saturation magnetization can be tolerated. From the measurements taken on these materials in L band, low field losses were apparent only for material no. 5, which exhibited a forward loss of 4.5 dB at 1.1 Gc.

Thus, in this band, material no. 4, whose operational characteristics produced a well-grouped impedance plot while operating in the low loss region, was considered the most promising material for the application of broadband matching techniques.

Material Evaluation, S-Band Region: The work done in the S-band region consisted of testing ferrimagnetic materials with various values of $4\pi M_s$ in a manner similar to the tests accomplished in the L-band region.

The $4\pi M_s$ values that were used for these tests were 200, 400, 670, and 1005 gauss which correspond to materials 2, 4, 5, and 6 listed in Table I.

All tests were conducted using a housing as shown in Fig. 1. Smith chart plots of the circulator using these materials were taken at various magnetic fields and are presented in Figs. 6 through 9.

These data agree with the results obtained in L band in that, as the $4\pi M_s$ is increased, the impedance plots tend to coalesce. Measurements of the loss characteristics indicated that the material with the highest $4\pi M_s$ which could be used, and yet avoid low field losses, was number 6. In both bands, then, a high saturation magnetization was required for producing the type of tight impedance plot grouping which effectively permits broadband matching.

A similar materials evaluation was made covering the remaining portion of the 0.6–8.0 Gc band. The results obtained were similar to those presented in the L- and S-band tests, in that, the higher the $4\pi M_s$, the more tightly grouped were the impedance characteristics for a particular frequency range. Also, as the frequency increased, the required $4\pi M_s$ for tight grouping became higher. The results of this investigation are presented in Fig. 10, which shows the optimum values of $4\pi M_s$ and ferrite disk diameters for each frequency.

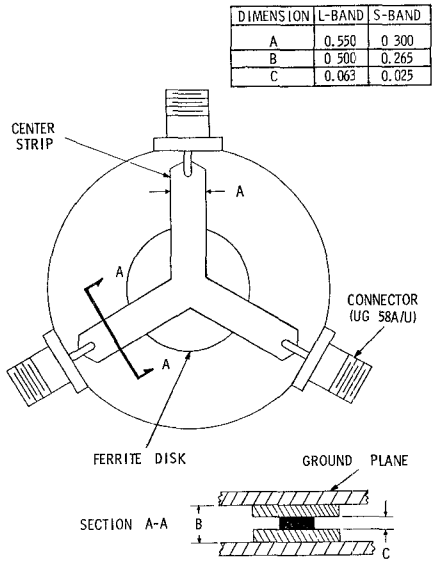

Fig. 1. Strip-transmission-line housing and ferrite configuration for the L- and S-band regions.

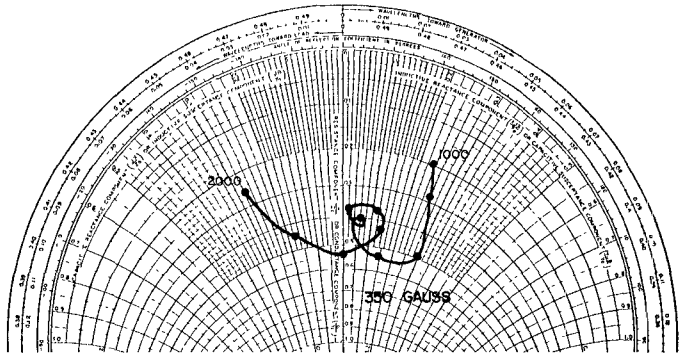

Fig. 4. L-band circulator impedance plot using material no. 4 ($4\pi M_s = 400$ gauss).

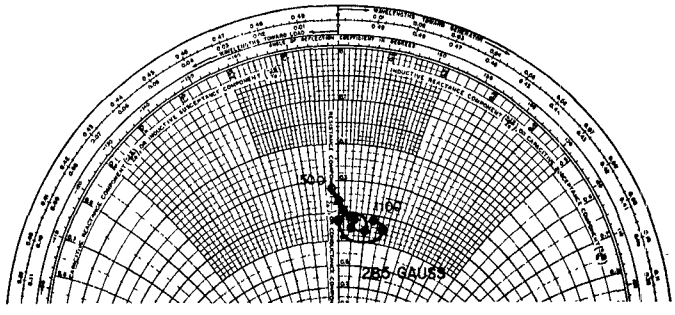

Fig. 5. L-band circulator impedance plot using material no. 5 ($4\pi M_s = 670$ gauss).

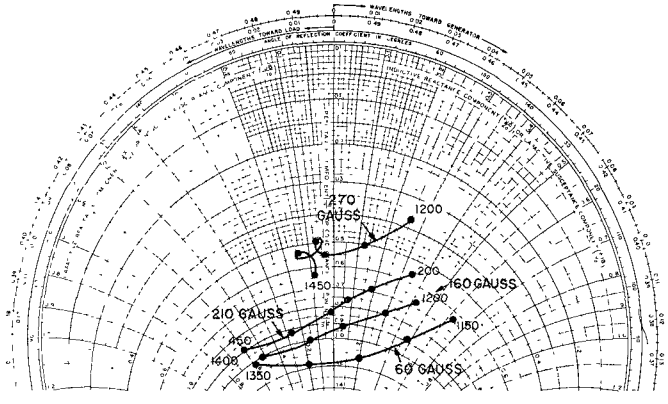

Fig. 2. L-band circulator impedance plot using material no. 1 ($4\pi M_s = 133$ gauss).

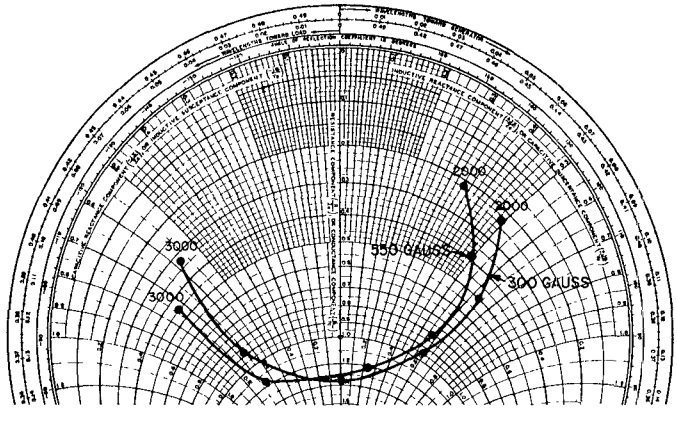

Fig. 6. S-band circulator impedance plot using material no. 2 ($4\pi M_s = 200$ gauss).

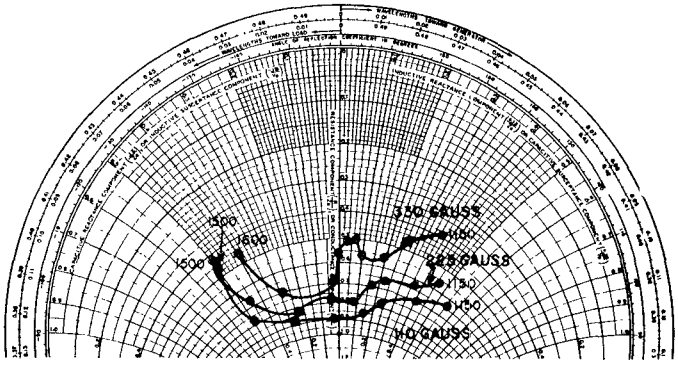

Fig. 3. L-band circulator impedance plot using material no. 2 ($4\pi M_s = 200$ gauss).

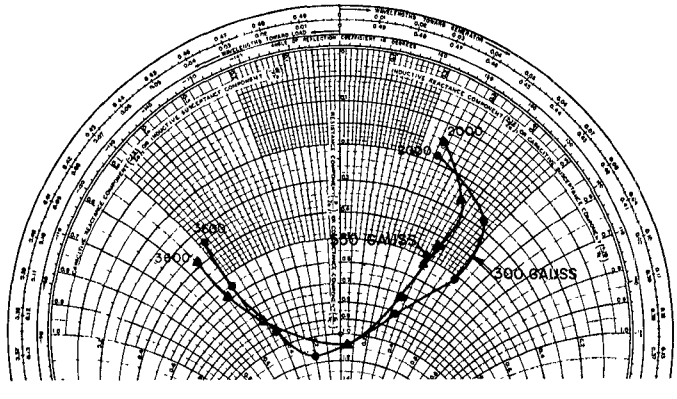

Fig. 7. S-band circulator impedance plot using material no. 4 ($4\pi M_s = 400$ gauss).

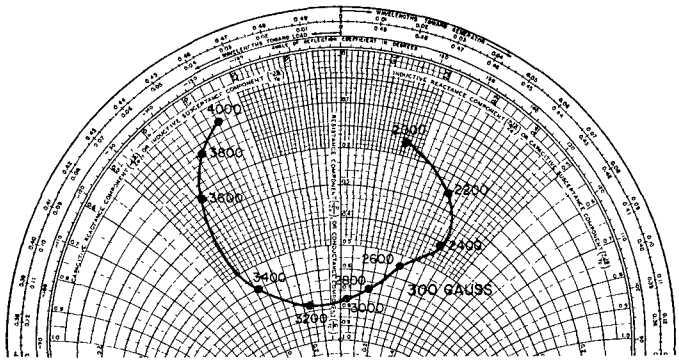

(a)

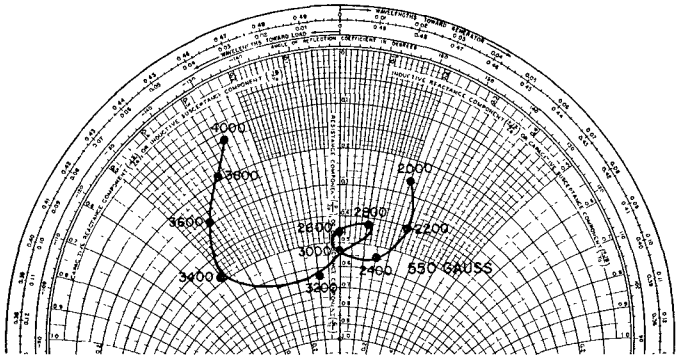

(b)

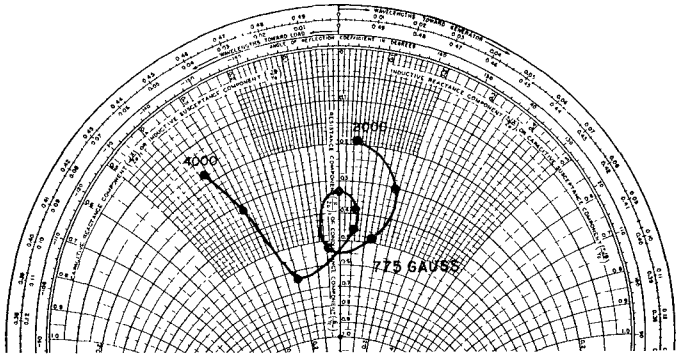

(c)

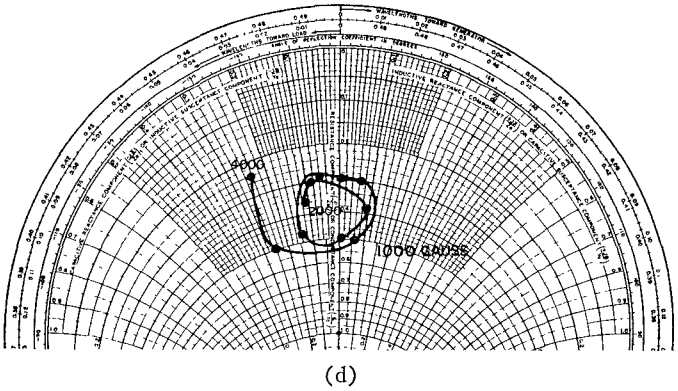

(d)

Fig. 8. *S*-band circulator impedance plot vs. magnetic field using material no. 5 ($4\pi M_s = 670$ gauss).

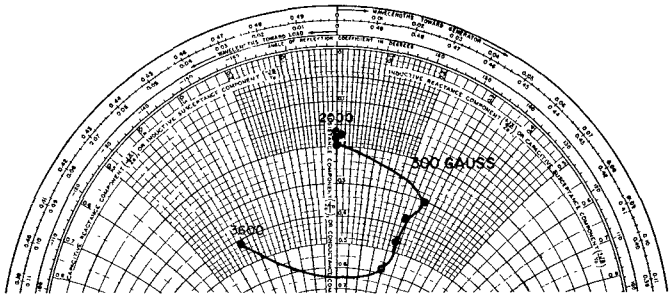

(a)

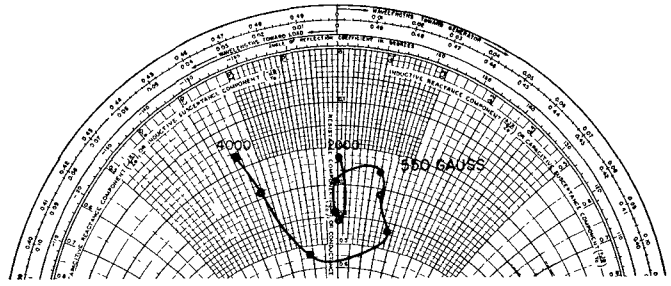

(b)

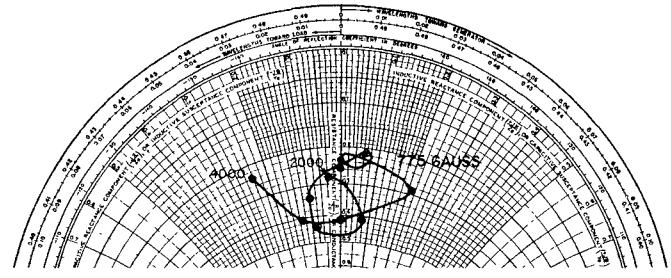

(c)

Fig. 9. *S*-band circulator impedance plot using material no. 6 ($4\pi M_s = 1005$ gauss).

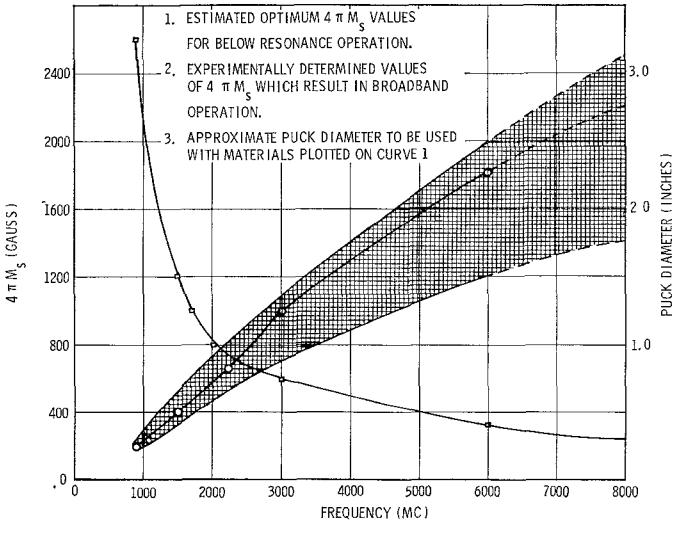

Fig. 10. Envelope of practical $4\pi M_s$ values and puck diameters for below resonance broadband operation.

Effects of Magnetic Field

The effects of varying the magnetic field are clearly illustrated in the impedance plots previously presented and are typical of all bands. It can be seen, for example, in Fig. 8(a) and 8(b) that the impedance becomes more tightly grouped as the applied field is increased; and at even higher fields, as shown in Fig. 8(c) and 8(d), the impedance plot continues to coalesce. However, as the field is increased the resonant frequency also increases, and a point is reached where high losses become evident on the lower end of the frequency band. In any given case, the resonance loss limits the extent to which the impedance plot can be coalesced by raising the applied field. In each band the optimum field was found to be approximately equal to the $4\pi M_s$ of the ferrite material.

Effects of Ferrite Geometry

Two examples are cited in Figs. 3 and 11 in which the impedance characteristics of the triangular- and disk-shaped garnet materials can be compared. In both cases, the similarity of the plots is surprisingly close. In the tests to date, no significant difference in the impedance characteristics for the disk or triangle has been found for any of the frequency bands or materials.

The disk-shaped ferrite, being easier to fabricate and smaller in size, was used in the development of these devices.

Effects of Dielectric Loss

The importance of using ferrimagnetic materials having low dielectric loss tangents, tan δ, can be simply illustrated through the use of experimental data taken recently in the L-band region. The materials used were numbers 3 and 4, respectively, whose only significant differences are in their dielectric loss tangents. The circulators containing the two materials were tuned and tested under similar conditions, and the results are plotted in Fig. 12(a) and 12(b). While the isolation and VSWR are quite similar, a noticeable drop of about 0.5 to 0.6 dB in the forward loss is evident for the material with the lower loss tangents in Fig. 12(b).

Thus, for circulators operating below resonance utilizing low saturation magnetization materials, and hence large disk diameters, dielectric loss is an important loss mechanism.

Effects of Linewidth

In choosing materials for possible below resonance operation, careful consideration must be given to the linewidth and frequency of operation. At the lower frequencies, where the field required for resonance becomes smaller and smaller and the tail of the resonance loss curve approaches the low field loss curve, the possible range of magnetic field values for low-loss operation becomes diminishingly small. This also becomes true at the higher frequencies where it is desirable to use the highest possible $4\pi M_s$ and biasing field. In either case, a narrow linewidth material has an appreciably larger operating region between the low field loss and the resonant loss region. From this standpoint, materials having the narrowest possible linewidths are desirable.

Materials have been tested which have all properties similar except linewidth. The results of these tests indicate that the linewidth has no measurable effect on the impedance characteristics of a circulator while operating in the low-loss region.

On the basis of these results, the linewidth of the material should be chosen to be as narrow as possible to permit the use of the highest possible saturation magnetization.

Effects of Strip-Transmission-Line Parameters

Only a limited amount of experimental data has been taken to study the specific function that stripwidth, strip thickness, characteristic impedance, etc., play in the bandwidth properties of circulators.

The strip-line configurations, which were used in the development of the circulators in the 1.0–2.0, 1.5–3.0, 2.0–4.0, and 4.0–8.0 Gc bands, are basically similar to Fig. 1. The ground plane spacings, stripwidth, and strip thickness were chosen to produce 50-ohm lines and also to suppress the propagation of higher order modes. This symmetrical Y-center conductor was used throughout the development described in the preceding paragraphs.

In the final stages of development of the 1.5–3.0 and 2.0–4.0 Gc bands, difficulty was encountered in obtaining a sufficiently good impedance grouping when using the material selected from the foregoing evaluation in a standard junction. Attempts were made to obtain an improved impedance plot by altering the center conductor geometry in the region of the junction. It became readily apparent from the experimental trials made that any *large* deviation from the straight Y configuration was detrimental to the impedance grouping. After a number of trials, some improvement was obtained by adding a slight taper to each leg entering the junction. Through this method, the necessary bandwidth was acquired for both bands.

In the 600–1200 Mc unit, a center conductor with a shielding disk [5] was found to be very useful for grouping the impedance characteristics. In this band, using material no. 2, at a constant magnetic biasing field of 190 gauss, a series of Smith chart plots was made for the following shield diameters: Straight Y (no shield), 0.800, 1.750, 2.000, 2.700, and 3.220 inches. The effects of the shield diameters are illustrated in Fig. 13. The two-inch-diameter shield was chosen to be used as the final design and later resulted in an octave bandwidth circulator.

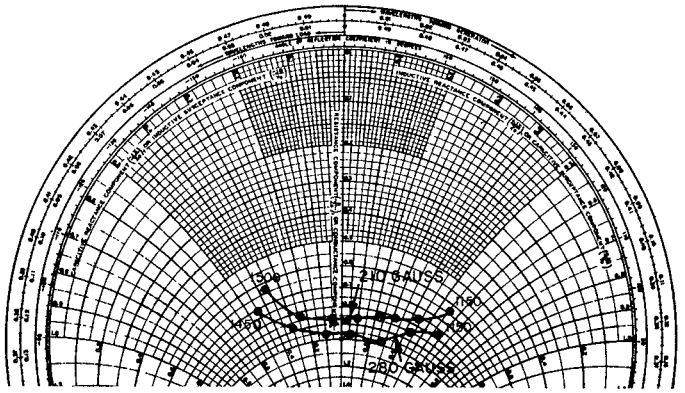

Fig. 11. L-band circulator impedance plot using material no. 2 (triangular-shaped ferrite element).

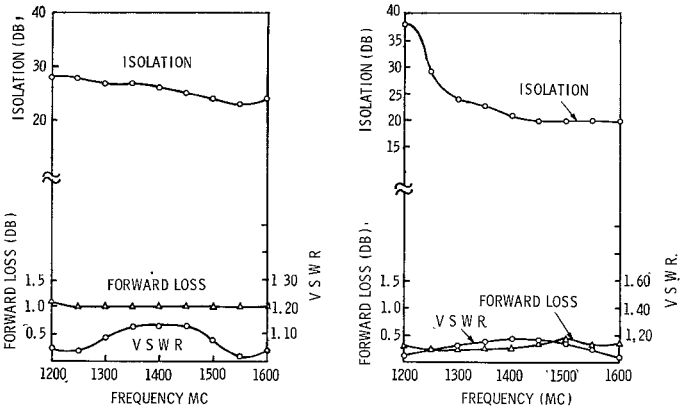

Fig. 12 (a) Loss characteristics of an L-band circulator using material no. 3 (tan $\delta = 0.002$). (b) Loss characteristics of an L-band circulator using material no. 4 (tan $\delta = 0.0001$).

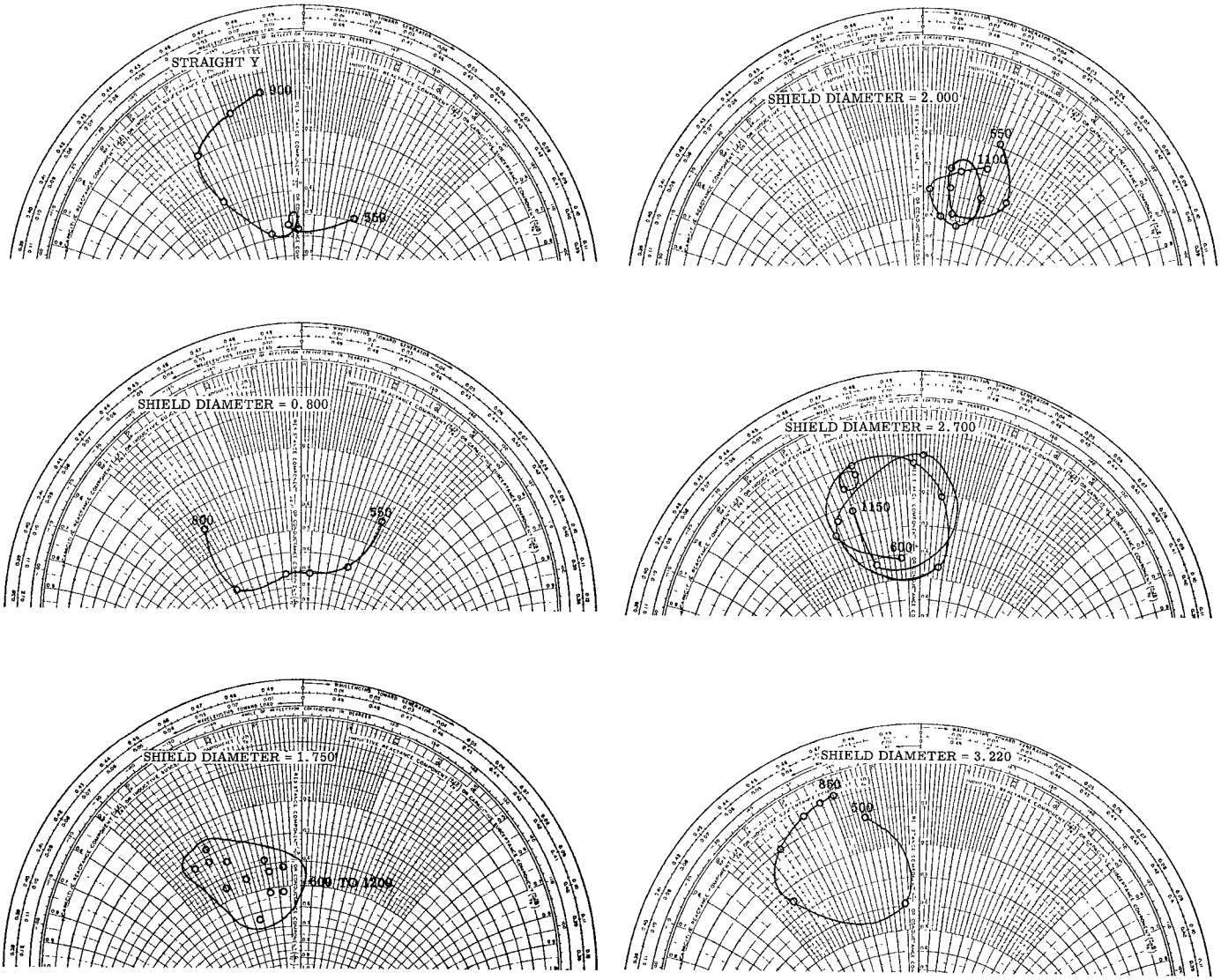

Fig. 13. UHF circulator impedance plots using a straight Y, 0.800, 1.750, 2.000, 2.700, and 3.220-inch shield diameters (material no. 2, biasing field = 190 gauss).

Octave Bandwidth Circulator Designs

Design Generation

From the results of the study just outlined, sufficient information is available for designing a circulator with impedance characteristics most favorably grouped for broadband matching. The steps to be followed in choosing optimum parameters are outlined below:

1) The choice of $4\pi M_s$ and ferrite disk diameter may be taken directly from Fig. 10.
2) The magnetic biasing field should be approximately equal to the $4\pi M_s$ of the material previously chosen, but can be adjusted in test for producing the best performance.
3) A ferrite material having a very low dielectric loss tangent is needed if low insertion loss is to be maintained.
4) The linewidth of the material must be narrow (approximately 50 to 100 Oe) if resonance losses are to be avoided.
5) In the strip-transmission-line structure, many combinations of stripwidth, strip thickness, and ground plane spacings may result in a broadband device. It is felt that the main consideration should be maintaining a 50-ohm line and preventing the propagation of higher order modes. Some guide in choosing the stripwidth, with relation to the ferrite disk diameter, can be obtained from Fig. 1.

After the optimization of the foregoing parameters, it becomes necessary to match these characteristics over octave bandwidths. The techniques that have been developed for all bands utilize common matching circuits. A description of some of these circuits and the results obtained are given later.

Specific Matching Techniques

In Fig. 4 an impedance plot of a 1.0–2.0 Gc circulator in the unmatched condition is shown. The grouping of this plot, as it stands, does not appear particularly good for broadband matching. However, if the output ports are matched to prevent re-reflections within the circulator, a surprisingly well-grouped plot results.

With the use of a double stub tuner inserted in the output arm (port 2), as shown in Fig. 14, the re-reflections between ports can essentially be eliminated by adjusting for maximum isolation between ports 1 and 3.

Using this technique for each of the frequency points, results were obtained as illustrated in Fig. 15. This plot now represents more accurately the impedance characteristic for which to design the matching element, since in the matched condition these internal reflections are very nearly canceled. The impedance response now looks very nearly like a low impedance resistive load.

The type of matching structure which has been used with greatest success, thus far, has been a single-element quarter-wavelength transformer located symmetrically in each arm. The function of this transformer is to match the 50-ohm line to the low impedance ferrite junction. With the use of this dielectric transformer, it was possible to obtain a good impedance match for 1.5–3.0, 2.0–4.0, and the 4.0–8.0 Gc units over an octave bandwidth.

In the development of the two lowest frequency units, difficulty was encountered in obtaining the full octave bandwidth using the quarter-wavelength matching transformers. The results of both units, when matched with the single transformer, are typically illustrated by the impedance plot shown in Fig. 16. This impedance plot is one which can be further improved by the addition of a resonant element having an impedance with an equal magnitude and an opposite phase slope. This type of circuit can be attained by the use of an open-circuited, quarter-wavelength stub in series with the strip-line center conductor. A stub of this type is equivalent to a series resonant circuit whose resonant frequency is controlled by the length of the stub. This circuit was built and tested in a separate housing, the results of which are shown in Fig. 17. With the addition of the resonant stub to the circulator, considerable improvement was obtained as shown in Fig. 18. A sketch of this resonant stub is shown in Fig. 19, and a photograph of the circuit built into the circulator is shown in Fig. 20.

Similar techniques were employed in improving the matched characteristics of the 1.0–2.0 Gc unit. The only parameter that required adjustment in using this stub in the 1.0–2.0 Gc band was the length of the wire stub.

Thus, in general, for achieving a sufficiently good match in any of the frequency bands, from 0.6–8.0 Gc, several techniques have been developed and demonstrated to be useful in matching the type of response which is characteristic of the below resonance circulator. With the use of these matching techniques and the information previously listed, octave bandwidth designs may be derived.

Electrical Performance

Typical data for the 0.6–1.2, 1.0–2.0, and 2.0–4.0 Gc units are shown in Figs. 21, 22, and 23. The performance of the 1.5–3.0 and 4.0–8.0 Gc units is quite similar to the 2.0–4.0 Gc circulator and will not be reproduced here. In some cases the relations between VSWR and isolation derived earlier do not hold in these illustrations. This variance is due to the ports being slightly unsymmetrical.

It should be noted that the high loss characteristics at the lower frequencies in Fig. 21 are probably a result of low field losses. With available ferrimagnetic materials, this type of loss mechanism is extremely difficult to avoid at frequencies as low as 0.600 Gc.

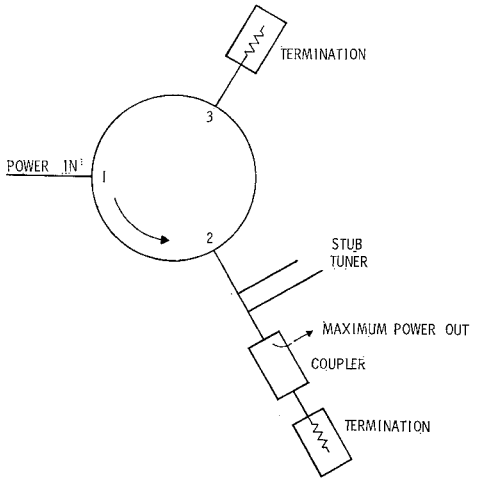

Fig. 14. The use of the double stub tuner for preventing re-reflections in circulator measurements.

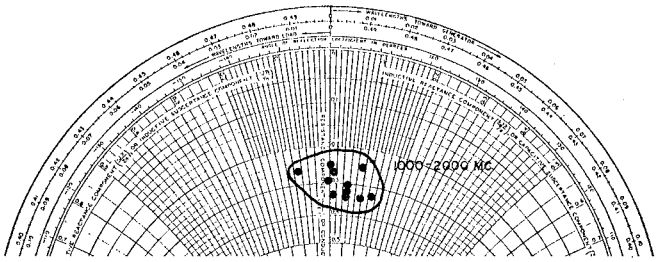

Fig. 15. *L*-band circulator impedance plot using material no. 4 with tuner in output arm.

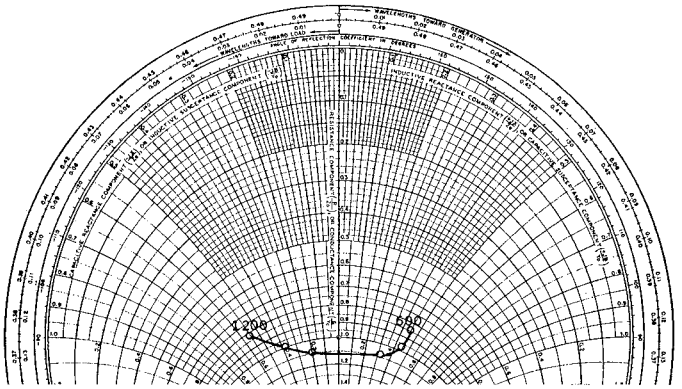

Fig. 16. Typical impedance characteristics of a 0.6–1.2 Gc circulator when matched with single-element dielectric transformers.

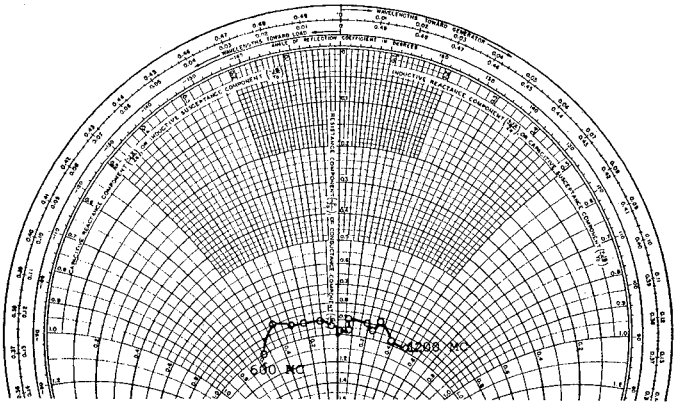

Fig. 17. Impedance characteristic of an open-circuited quarter-wavelength stub when tested in a 50-ohm line.

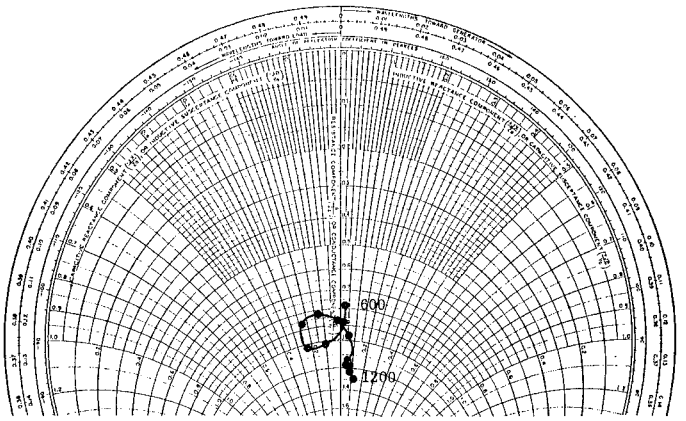

Fig. 18. Impedance characteristic of a 0.6–1.2 Gc circulator when matched with a resonant stub.

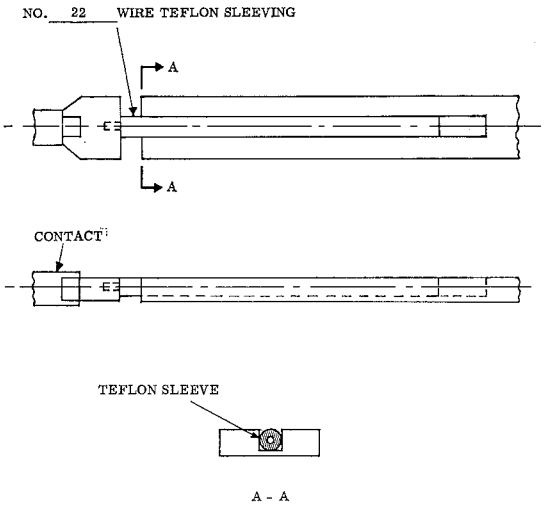

Fig. 19. Sketch of the open-circuited stub mounted in series with the strip-line center conductor.

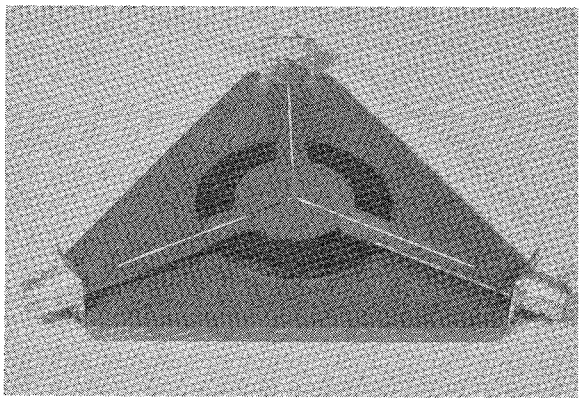

Fig. 20. Photograph illustrating the location of the resonant circuit.

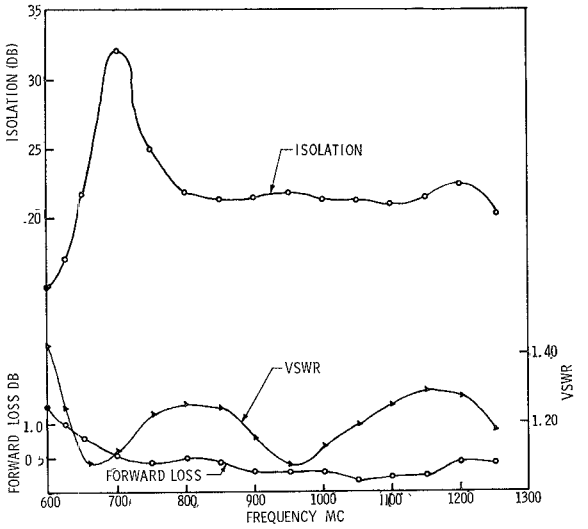

Fig. 21. UHF circulator characteristics.

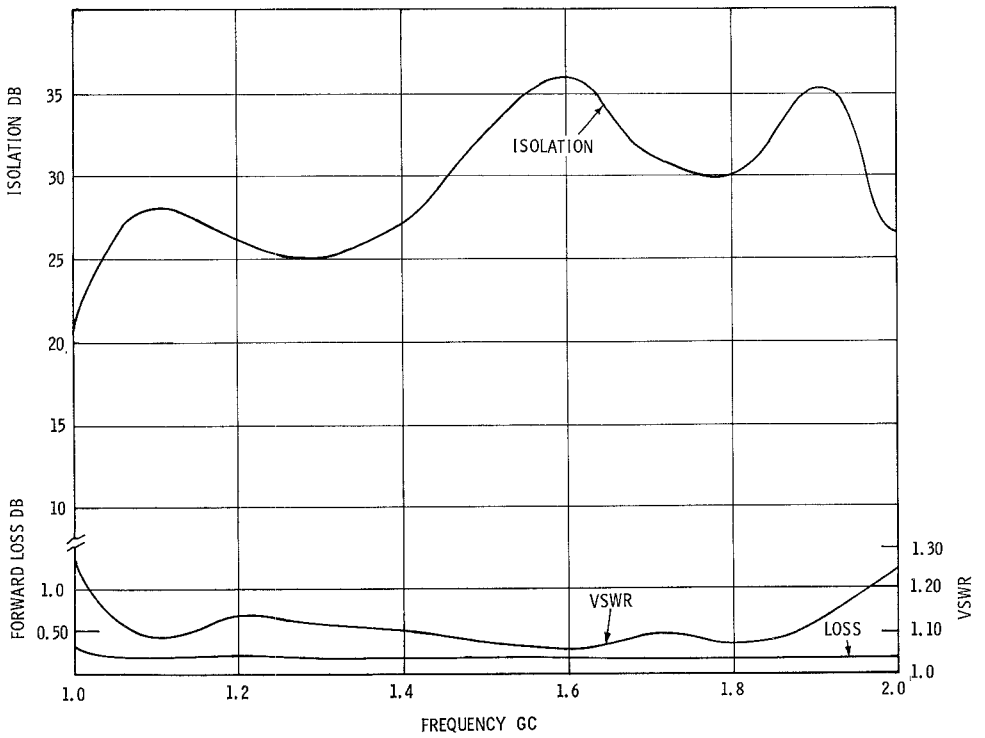

Fig. 22. Octoave bandwidth operating characteristics of the 1.0–2.0 Gc circulator.

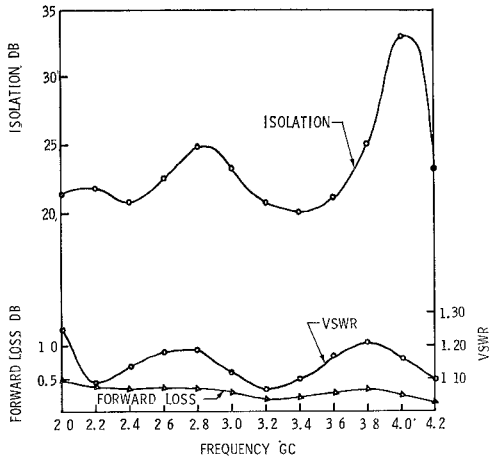

Fig. 23. Characteristics of a typical *S*-band circulator.

Conclusions

The most important single factor in contributing to the development of the broadband circulators was the discovery of the strong dependence of the impedance characteristics upon the saturation magnetization. Once the optimum $4\pi M_s$ is established, the parameters of secondary importance such as magnetic field, strip thickness, stripwidth, ground plane spacing, matching techniques, etc., can be carefully adjusted for attaining maximum bandwidth.

Although a great deal has been accomplished in broadbanding circulators by empirically optimizing the saturation magnetization and developing the appropriate matching techniques, it is presently felt that greater bandwidths are attainable. A likely means of accomplishing this end is through the use of multiple-element matching transformers and through improved center conductor geometries that can be developed experimentally.

Appendix I

An interesting theoretical result that confirms what has been observed experimentally for some time with regard to the relation between isolation and VSWR in a circulator is derived in this section.

It is well known [9] that a lossless *reciprocal* three-port junction cannot be matched out. This is easily shown as follows: If the junction is matched and reciprocal, the scattering matrix must be of the form:

$$\mathcal{S} = \begin{pmatrix} 0 & S_{21} & S_{31} \\ S_{21} & 0 & S_{32} \\ S_{31} & S_{32} & 0 \end{pmatrix}. \tag{1}$$

If, in addition, it is lossless, the following equations must hold:

$$S_{21}S_{32*} = S_{21}S_{31*} = S_{31}S_{32*} = 0. \tag{2}$$

$$|S_{21}|^2 + |S_{31}|^2 = |S_{21}|^2 + |S_{32}|^2 = 1. \tag{3}$$

There does not exist a set of values satisfying (2) and (3) since this would require one of the elements to be zero and, at the same time, have an absolute value of unity, which obviously cannot be. Hence, a reciprocal lossless three-port junction cannot be matched.

One can arrive at essentially the same result from a different point of view. If the three-port junction is required to be symmetric, then the scattering matrix can be of the form:

$$\mathcal{S} = \begin{pmatrix} S_{11} & S_{31} & S_{21} \\ S_{21} & S_{11} & S_{31} \\ S_{31} & S_{21} & S_{11} \end{pmatrix}. \tag{4}$$

If the junction is also to be matched, then the matrix must be of the form:

$$\mathcal{S} = \begin{pmatrix} 0 & S_{31} & S_{21} \\ S_{21} & 0 & S_{31} \\ S_{31} & S_{21} & 0 \end{pmatrix} \tag{5}$$

and if the junction is lossless, then it is seen that

$$|S_{21}| = 1 \quad \text{and} \quad S_{31} = 0 \tag{6}$$

or

$$S_{21} = 0 \quad \text{and} \quad |S_{31}| = 1. \tag{7}$$

Condition (6) gives a junction that circulates in the mode, port 1→port 2→port 3→port 1 (1→2→3→1), and condition (7) gives one that circulates in the mode (1→3→2→1). Hence, a matched symmetric, lossless three-port junction is necessarily a circulator. Also, this shows that the procedure of matching out ports in the laboratory is precisely equivalent to building a circulator; a result that was also obtained from the solution of the boundary-value problem using Bosma's boundary conditions [5].

It has been observed for some time that, if one determines the VSWR for each of the ports of a Y junction and if the VSWR's are relatively small (e.g., less than 1.5), then the isolation of port 3, when power is put in port 1, will be equal to the VSWR of port 2 when converted to decibels. This is true provided the junction is tending to circulate in the 1→2→3→1 mode. If circulation is in the mode 1→3→2→1, obvious changes in the foregoing statement are required. This result can be obtained theoretically as follows. Consider the scattering matrix for a general three-port junction:

$$\mathcal{S} = \begin{pmatrix} S_{11} & S_{12} & S_{13} \\ S_{21} & S_{22} & S_{23} \\ S_{31} & S_{32} & S_{33} \end{pmatrix}. \tag{8}$$

If the VSWR's of all ports are small, this requires

$$|S_{ii}| \ll 1 \qquad \text{for } i = 1, 2, 3. \tag{9}$$

If the Y junction is tending to circulate in the 1→2→3→1 mode, then

$$|S_{31}|, \quad |S_{12}|, \quad |S_{23}| \ll 1 \tag{10}$$

and

$$|S_{21}| \doteq |S_{32}| \doteq |S_{13}| \doteq 1. \tag{11}$$

It is necessary to assume the junction has low loss in order to obtain (11). If it has low loss, then

$$S_{11}S_{12*} + S_{21}S_{22*} + S_{31}S_{32*} \doteq 0. \tag{12}$$

Since $S_{11}S_{12*}$ is small to the second order and $|S_{21}| \doteq |S_{32}| \doteq 1$ to first order, it follows that to first order we have

$$|S_{22}| = |S_{31}|. \tag{13}$$

According to (13), if power $|A|^2$ enters port 1, then power $A^2|S_{31}|^2$ will come out port 3, and if power A^2 is put in port 2, power $|A|^2|S_{22}|^2=|A|^2|S_{31}|^2$ will be reflected. This is precisely the result sought.

A special case of this result, obtained by Aitken and McLean [8], states that, if the junction is symmetric, the power reflected at port 1 and the power out port 3 will be equal. This follows since, if the junction is symmetric, $S_{11}=S_{22}$ and $|A|^2|S_{31}|^2=|A|^2|S_{11}|^2$.

The fact that the derivation of (13) did not require symmetry makes the result particularly useful to the experimentalist since he will, in general, be dealing with junctions that are not truly symmetric.

Acknowledgment

The author wishes to acknowledge the assistance of W. Passaro and D. Landry in the development of these devices and Dr. G. Burdick, who contributed greatly in providing the theoretical background and guidance throughout the program.

References

[1] Milano, U., J. H. Saunders, and L. Davis, Jr., A Y-junction strip-line circulator, *IRE Trans. on Microwave Theory and Techniques*, vol MTT-8, May 1960, pp 346–350.
[2] Clark, J., Perturbation techniques for miniaturized coaxial Y-junction circulators, *J. Appl. Phys.*, suppl. to vol 32, Mar 1961, p 323s–324s.
[3] Clark, J., and J. Brown, Miniaturized, temperature stable coaxial Y-junction circulators, *IRE Trans. on Microwave Theory and Techniques*, vol MTT-9, May 1961, pp 267–269.
[4] Auld, B. A., The synthesis of symmetrical waveguide circulators, *IRE Trans. on Microwave Theory and Techniques*, vol MTT-7, Apr 1959, pp 238–246.
[5] Bosma, H., On the principle of stripline circulation, *Proc. IEE (London)*, vol 109, pt B, suppl. no 21, Jan 1963, p 137–146.
[6] ——, On stripline Y-circulation at UHF, *IEEE Trans. on Microwave Theory and Techniques*, vol MTT-12, Jan 1964, pp 61–72.
[7] Humphreys, B. L., and J. B. Davies, The synthesis of N-port circulators, *IRE Trans. on Microwave Theory and Techniques*, vol MTT-10, Nov 1962, pp 551–554.
[8] Aitken, F. M., and R. McLean, Some properties of the waveguide Y-circulator, *Proc. IEE (London)*, Feb 1963, pp 256–260.
[9] Montgomery, C., R. H. Dicke, and E. M. Purcell, *Principles of Microwave Circuits*. New York: McGraw-Hill, 1948, ch 12.

Generalized Plots of Mode Patterns in a Cylindrical Dielectric Waveguide Applied to Retinal Cones

G. BIERNSON, SENIOR MEMBER, IEEE, AND D. J. KINSLEY

Abstract—**Generalized curves are presented which describe the characteristics of the 12 lowest cutoff-frequency modes of an electromagnetic wave propagating down an infinite lossless dielectric rod, surrounded by an infinite lossless medium of lower dielectric constant. These curves were developed by a computer study particularly to analyze the optical mode patterns generated within the photosensitive portions of the cones of the retina. However, they should also be particularly useful in the study of fiber optics and dielectric microwave antennas.**

I. Introduction

A DIELECTRIC rod surrounded by a medium of lower dielectric constant acts as a waveguide. However, the characteristics of the modes propagated in such a waveguide are more complex than in the more familiar metallic waveguide case because 1) part of the energy propagates outside the dielectric rod, and 2) the spatial distribution of the energy in a mode varies with wavelength. In a metallic waveguide, all the energy is contained within the waveguide, and the shape of a mode is the same over the frequency range at which it can exist.

Stratton [1] has shown that the characteristics of the modes can be obtained by solving a complicated transcendental equation containing Bessel and Hankel functions. Snitzer [2] has discussed the nature of the modes which arise from solutions of this equation. This paper presents the results of a digital computer solution of this equation, which has provided a series of generalized curves describing the characteristics of the 12 modes having the lowest cutoff frequencies. This approach can be extended to include other modes. The spatial distribution of energy in a given mode is characterized by a Bessel function of a particular order. For each mode, the Bessel-function argument at the boundary of the rod (designated u) is plotted vs. a nondimensional fre-

Manuscript received August 3, 1964; revised February 1, 1965. The work reported herein was sponsored under contract AF-33(657)-11717 with the Aerospace Medical Research Laboratories, Air Force Systems Command, U. S. Air Force.

The authors are with the Applied Research Lab., Sylvania Electronic Systems, a Div. of Sylvania Electric Products Inc., Waltham, Mass.